JM PAPERS

Subcritical transitional flow in two-dimensional plane Poiseuille flow

Z. Huang[1], R. Gao[1], Y.Y. Gao[1] and G. Xi[1],†

[1]Department of Fluid Machinery and Engineering, Xi'an Jiaotong University, Xi'an 710049, PR China

Recently, subcritical transition to turbulence in the quasi-two-dimensional (quasi-2-D) shear flow with strong linear friction (Camobreco *et al.*, *J. Fluid Mech.*, vol. 963, 2023, R2) has been demonstrated by the 2-D mechanism at $Re = 71\,211$, and the nonlinear Tollmien–Schlichting (TS) waves related to the edge state were approached independently of initial optimal disturbances. For 2-D plane Poiseuille flow, transition to the fully developed turbulence requires that the Reynolds number is several times larger than the critical Reynolds number Re_c (Markeviciute & Kerswell, *J. Fluid Mech.*, vol. 917, 2021, A57). In this paper, we observed the subcritical transitional flow in 2-D plane Poiseuille flow driven by the nonlinear TS waves by both linear and nonlinear optimal disturbances ($Re < Re_c$) with different quantitative edge states. The nonlinear optimal disturbances could trigger the sustained subcritical transitional flow for $Re \geqslant 2400$. The initial energy for nonlinear optimal disturbance is more efficient than the linear optimal disturbance in reaching the subcritical transitional flow for $2400 \leqslant Re \leqslant 5000$. Moreover, the initial energy of linear optimal disturbance is larger than the energy of its edge state. The nonlinear TS waves along the edge state are formed by the nonlinear optimal disturbances to trigger transitional flow, which agrees well with the main conclusions of Camobreco *et al.* (*J. Fluid Mech.*, vol. 963, 2023, R2), while the required Re of 2-D plane Poiseuille flow is much smaller.

Key words: nonlinear instability, shear-flow instability

1. Introduction

Subcritical transition to turbulence has received much attention for many decades since the linear stability theory based on unstable eigenvalues (Lin 1944) could not explain the transition to turbulence observed by the classic experiments (Reynolds 1883; Davis & White 1928; Tillmark & Alfredsson 1992). The short-term instability behaviour treated as transient growth of the finite amplitude optimal disturbances illustrated an optional

† Email address for correspondence: xiguang@mail.xjtu.edu.cn

transition scenario for linear stable flows. Therefore, theoretical (Trefethen & Embree 2005; Schmid 2007) and numerical (Butler & Farrell 1992) studies on transient growth have been performed to describe the subcritical transition to turbulence.

The linearized Navier–Stokes (NS) equations for shear flows are employed to seek the optimal disturbances that experience possible largest amplification. Mathematically, the non-orthogonality of the eigenvectors or pseudospectra induce the instabilities (Trefethen & Embree 2005); while physically the optimal disturbances could be amplified by the Orr and lift-up mechanisms in shear flows (Schmid 2007). According to the non-normal analysis, the disturbance energy increases linearly with Reynolds number *Re* and the short-term target time for parallel shear flows. For three-dimensional (3-D) shear flows, the optimal disturbances are amplified by the lift-up mechanism to form streaks, achieving greater than a thousandfold growth in energy. According to the linear instability analysis, the two-dimensional (2-D) plane shear flow is the most unstable due the occurrence of Tollmien–Schlichting (TS) waves. However, for 2-D linear stable shear flows, the energy is amplified tenfold rapidly via the Orr mechanism. Therefore, the 3-D optimal disturbances are popular for investigating the subcritical transition to turbulence (Butler & Farrell 1992; Reddy *et al.* 1998; Chapman 2002; Karp & Cohen 2014; Farano *et al.* 2015*b*; Roizner, Karp & Cohen 2016) due to considerable transient growth as a primary instability. The TS waves and the optimal streaks are considered together in plane Poiseuille flow (Zammert & Eckhardt 2019), they found that the lower branch solution of the TS wave solution bifurcating from the base flow, is an edge state of the 3-D system and 2-D system for a range of *Re*.

Interestingly, the Orr and lift-up amplifications could be combined to drive the optimal disturbances in shear flows. Non-parallel shear flow, such as spatially developing boundary layer flows, enable the linear optimal disturbances to be amplified by the Orr and lift-up mechanisms simultaneously (Hack & Moin 2017). Furthermore, the nonlinearity combines the two mechanisms to result in much larger energy growth for parallel shear flows (Pringle & Kerswell 2010), which is more important for investigating the subcritical transition of shear flows quantitatively. For 3-D parallel shear flows, the nonlinear optimal disturbances are localized wave packets that are tilted against the mean shear. The disturbances are unpacked and amplified by the Orr mechanism to obey the shear firstly, and forming the streamwise streaks by nonlinear oblique interactions and the lift-up mechanism, before triggering the subcritical transition to turbulence (Cherubini *et al.* 2011; Monokrousos *et al.* 2011; Pringle, Willis & Kerswell 2012; Rabin, Caulfield & Kerswell 2012; Eaves & Caulfield 2015). The coherent structures are streaks for the edge state along the basin boundary between the laminar and turbulent attractors for 3-D parallel shear flows (Kerswell 2018).

However, the mechanism of subcritical transition to turbulence in 2-D shear flows has remained mysterious, until the very recent quasi-2-D shear flow investigation by Camobreco, Pothérat & Sheard (2023). The subcritical transition pathway from the laminar to the turbulent state, i.e. the nonlinear TS waves, has been found by the linear optimal disturbances. Although the subcritical lift-up transition is greatly suppressed in the quasi-2-D shear flow, the small-scale turbulence was achieved eventually. It is very hard to observe subcritical transition to turbulence in 2-D shear flows since the 2-D turbulence manifests quite differently from the 3-D turbulence, such as the reverse energy cascade (Boffetta & Ecke 2012). In fact, the fully developed turbulence in 2-D plane Poiseuille flow could not be obtained until Reynolds numbers were far beyond the critical value Re_c (Falkovich & Vladimirova 2018; Markeviciute & Kerswell 2021). Therefore, the subcritical transition to turbulence still remains an open question for pure 2-D plane

Poiseuille flow, including reaching the 2-D turbulent state, the critical *Re*, the efficient optimal disturbances and the edge states.

The study (Camobreco *et al.* 2023) mainly discussed the subcritical transition mechanism along the same edge state touched by alternative linear optimal disturbances at $r_c = Re/Re_c = 0.9$ ($Re = 71\,211$) with the strong linear friction. However, the edge state introduced in nonlinear non-modal analysis (Kerswell 2018) represents the basin boundary for transitional flow quantitatively and usually relates to the minimal seed. Moreover, the quantitative optimal disturbances and critical *Re* are of valuable interest to trigger turbulence for 2-D shear flows, such as electron fluid (Sulpizio *et al.* 2019) with high performance. In this study, we performed both the linear and nonlinear optimization to seek the efficient optimal disturbances that experience nonlinear TS waves along the edge state to trigger subcritical transition to turbulence in 2-D plane Poiseuille flow. Instead of the 2-D fully turbulent state, the chaotic transitional flow is obtained by both linear and nonlinear optimal disturbances via quantitatively different edge states. The critical *Re* is approximately 2400 for the subcritical transitional flow due to the nonlinear TS waves. The nonlinear disturbances are also wall modes for large *Re*, similar to linear optimal disturbances; while for small *Re*, the nonlinear optimal disturbances deviate the wall mode.

In the material that follows, §2 describes the governing equations and numerical method, followed by the discussion of subcritical transitional flow in §3. Section 4 illustrates the wall mode optimal disturbances for subcritical transitional flow, and the discussion and conclusions are presented in §5.

2. Governing equations and numerical simulations

The 2-D plane shear flow is governed by the incompressible NS equations

$$U_t + U \cdot \nabla U = -\nabla P + \frac{1}{Re}\nabla^2 U, \quad \nabla \cdot U = 0, \tag{2.1a,b}$$

where U is the velocity vector (U, V), and P is the pressure. Let the laminar state of plane channel flow $U = (U(y), 0)$, and for the plane Poiseuille flow $U(y) = 1 - y^2$. The equations are non-dimensionalized by the maximum velocity U_{max}, half-height of the channel h, time h/U_{max}, and pressure ρU_{max}^2. The Reynolds number $Re = U_{max}h/\nu$, where ν is the viscosity. The perturbation velocity vector is $u = u_{tot} - U$. Therefore, the governing equations of the perturbation velocities are

$$u_t + u \cdot \nabla U + u \cdot \nabla u + U \cdot \nabla u = -\nabla p + \frac{1}{Re}\nabla^2 u, \quad \nabla \cdot u = 0. \tag{2.2a,b}$$

Falkovich & Vladimirova (2018) found the pressure-driven laminar flow induces travelling waves for sufficiently small viscosity and friction. By adding uniform friction to real fluid layers, the turbulent flow was observed at $Re \sim 30\,000$ much larger than $Re_c = 7696$, which is based on the flow rate ($4/3U_{max}$). The subcritical transition to turbulence in quasi-2-D flows has been studied in the duct flows with moving walls driven by the linear friction under a strong transverse magnetic field (Camobreco *et al.* 2023). Due to the significant effect of linear friction, the critical Reynolds number $Re_c = 79123.2$, which is based on the half-duct-height and the maximum velocity U_{max} in Camobreco, Pothérat & Sheard (2021). They calculated the linear optimizations for the quasi-2-D shear flow in a rectangular duct with significant linear friction under a strong magnetic field at $Re = 71\,211$, and found the linear and nonlinear optimizations offer identical results to approach the edge state. However, the nonlinear optimal disturbances with the minimal

energy, or the so-called minimal seeds (Pringle *et al.* 2012; Eaves & Caulfield 2015), are the perfect choice to trigger the subcritical transition along the edge state between the nonlinear laminar and turbulent attractor basin boundary. Therefore, besides the linear optimizations, we employed fully nonlinear optimizations to investigate the subcritical transition via the nonlinear edge state for 2-D plane Poiseuille flow. The nonlinear optimal disturbance and the related evolution in the channel could be identified by the variational method (see Pringle & Kerswell (2010), Cherubini *et al.* (2011) and Monokrousos *et al.* (2011)). The disturbance energy density is defined as

$$E(t) = \frac{1}{2V} \int_V [u^2(t) + v^2(t)] \, dV, \quad (2.3)$$

and energy density of streamwise and vertical velocity disturbances

$$E_u(t) = \frac{1}{2V} \int_V u^2(t) \, dV, \quad E_v(t) = \frac{1}{2V} \int_V v^2(t) \, dV, \quad (2.4a,b)$$

where V is the volume of the channel, and for 2-D flow $V = 2hLx$ is the area of the channel. By defining the objective functions and introducing the Lagrangian multipliers, the adjoint governing equations are formulated as

$$u^\star_t + u \cdot \nabla u^\star - u^\star \cdot \nabla u = -\nabla p^\star - \frac{1}{Re} \nabla^2 u^\star, \quad \nabla \cdot u^\star = 0, \quad (2.5a,b)$$

where $u^\star$ is the adjoint velocity of disturbance velocity u, and $p^\star$ is the adjoint variable of pressure disturbance p.

There are many numerical optimized methods to seek the nonlinear optimal disturbance for shear flows (Pringle & Kerswell 2010; Monokrousos *et al.* 2011; Cherubini & Palma 2015; Huang & Philipp 2020). In order to capture the edge state of subcritical transition, the disturbance energy density (Pringle & Kerswell 2010) and the total time-averaged dissipation are defined (Monokrousos *et al.* 2011) as the objective function, respectively. In this study, the nonlinear optimizations are conducted by the well-developed direct-adjoint-looping method based on the direct numerical simulation (DNS) codes Diablo (Taylor 2008). The Fourier truncations are used in the streamwise x-direction, and the dealiasing technique which removes the highest $1/3$ portion of the Fourier spectrum is employed. The finite difference method is used for the spatial discretizations in the wall-normal direction, and a combined implicit–explicit Runge–Kutta–Wray Crank–Nicolson scheme for time integration. The numerical energy threshold could be obtained by the bisection technique. Since the simulated turbulence effects are very strong for long 2-D channels (Jiménez 1987, 1990), the wavenumber $\alpha_{domain} = 0.1$ is mainly considered to define the computational domain length $Lx = 2\pi/\alpha_{domain} = 20\pi$, and α is used for convenience and refers to the channel length if not specified in this study. According to Jiménez (1990), the target time $T = 2000$ is sufficient to observe the saturated nonlinear interactions for 2-D plane Poiseuille flow. The edge tracking method is shown in figure 1, the edge state is bracketed by energy trajectories of red solid and dashed lines with initial energy density of 9.24967×10^{-6} and 9.24965×10^{-6}, respectively, for $Re = 3500$. Therefore, for convenience, we only show the two bounded trajectories in this paper. The edge tracking technique is very similar to that shown in figure 1 in Zammert & Eckhardt (2014). We performed the grid sensitivity study with three grid resolutions, i.e. 512×256, 1024×512 and 2048×1024, the corresponding critical energy densities that induce the subcritical transitional flow are 1.025×10^{-5}, 9.2497×10^{-6} and 9.241×10^{-6}, respectively. The energy relative difference between
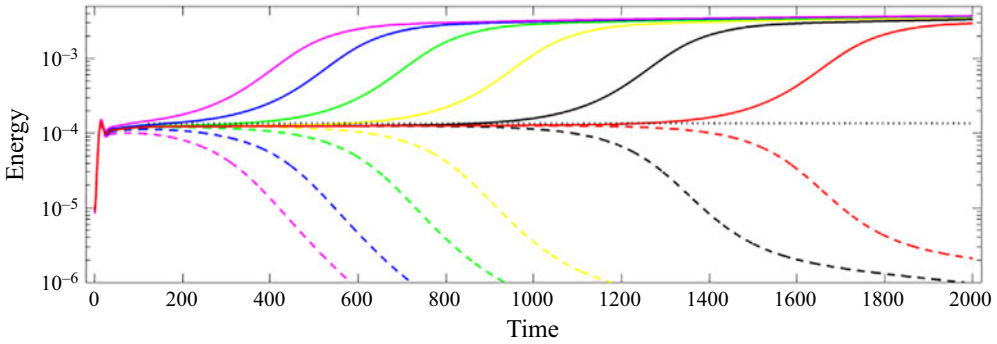
Figure 1. The edge tracking in 2-D plane Poiseuille flow at $Re = 3500$: the solid lines are the initial densities of trajectories that trigger subcritical transition; the dashed lines are trajectories of laminar; and the edge state (dotted line) bracketed by the trajectories of red lines.

the grids 1024×512 and 2048×1024 is less than 0.1 %. Therefore, the grid resolution 1024×512 is employed with more than 256 points distributed near the channel walls within $h/4$. The time step 0.01 is chosen for all numerical optimizations and DNS in this study.

3. Subcritical transitional flow

According to the linear stability analysis, the critical Reynolds number Re_c is approximately 5772.2 for 2-D plane Poiseuille flow (Orszag 1971). Figures 2(*a*) and 2(*b*) compare the time variation of kinetic energy of linear and nonlinear optimal disturbances at the subcritical Reynolds number $Re = 3500$ for different channel lengths. The linear optimal disturbances in this study are calculated for the maximal transient energy growth. For example, the maximal energy gain is 34.08 with optimal target time $T_{opt} = 12.55$ with optimal wavenumber of 1.53 at $Re = 3500$. We calculated the linear optimal disturbances with target time T_{opt} by the numerical optimization (Butler & Farrell 1992), while the nonlinear optimal disturbances are captured for $T = 2000$. Both of the optimal disturbances could reach the chaotic transitional flow via their edge states of different energy norms with different channel length, as shown in figures 2(*a*) and 2(*b*). For linear optimal disturbances, the initial energies are rescaled up to $E_0 = 1.44909 \times 10^{-3}$ and $E_0 = 4.076686 \times 10^{-4}$ for $\alpha = 0.4$ and $\alpha = 0.1$, respectively, to trigger the chaotic transitional flow via the edge state related to the energy plateau; while the flows are finally relaminarized after the experienced edge states for $E_0 = 1.449085 \times 10^{-3}$ and $E_0 = 4.076684 \times 10^{-4}$. The energy norm of the edge state is approximately 2×10^{-3}, which is larger than the initial energy for $\alpha = 0.4$. While the energy norm of edge state is approximately 2×10^{-4}, which is much smaller than the initial energy for $\alpha = 0.1$. The linear optimal disturbances experience amplification, decay in an oscillatory way and then monotonically to touch the edge state. For the nonlinear optimal disturbances, or minimal seeds, the critical initial energies are $E_0 = 3.602621 \times 10^{-5}$ and $E_0 = 9.24967 \times 10^{-6}$ for $\alpha = 0.4$ and $\alpha = 0.1$, respectively. The required energies of nonlinear optimal disturbances are approximately 2.5 % of those of linear optimal disturbances for both $\alpha = 0.4$ and $\alpha = 0.1$. The minimal seeds are amplified rapidly and decay to the edge states, whose energy norms are approximately 7.0×10^{-4} and 1.25×10^{-4} for $\alpha = 0.4$ and $\alpha = 0.1$, respectively, before reaching the transitional flow.
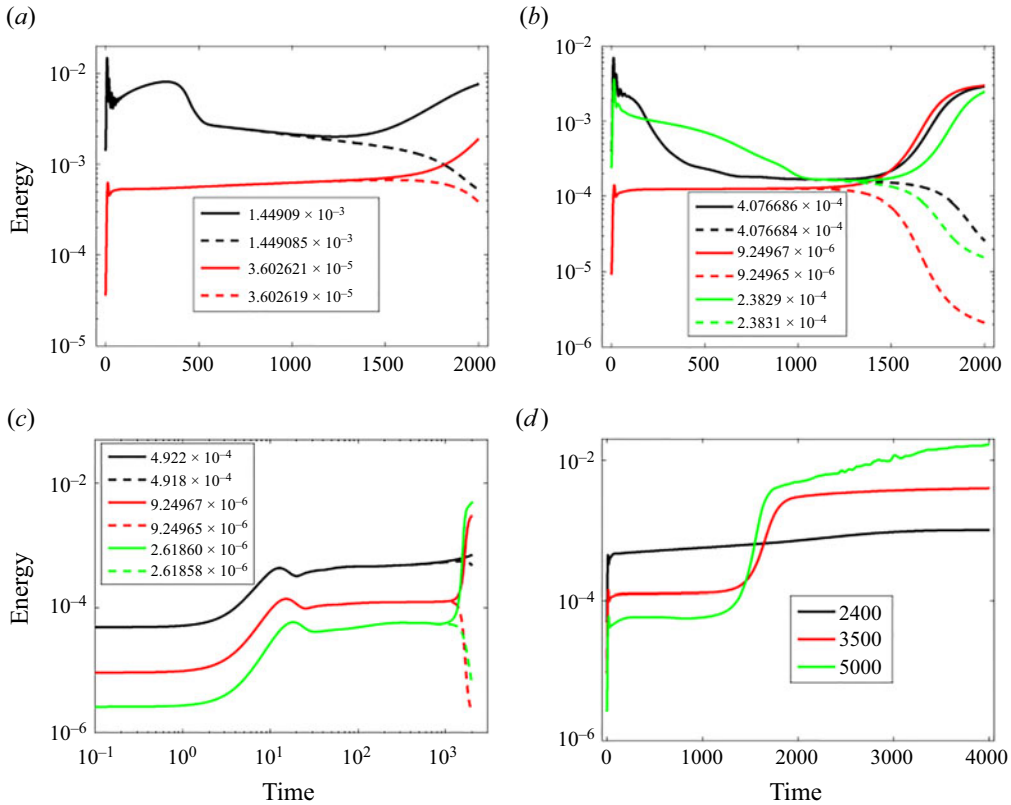
Figure 2. (*a*) The time history of perturbation kinetic energy for linear (black lines) and nonlinear (red lines) optimal disturbances at $Re = 3500$ and $\alpha = 0.4$. (*b*) The time history of perturbation kinetic energy for linear (black lines for T_{opt} and green lines for $10T_{opt}$) and nonlinear (red lines) optimal disturbances at $Re = 3500$ and $\alpha = 0.1$. (*c*) The time variation of perturbation kinetic energy of nonlinear optimal disturbances for different Re; the black, red and green lines are corresponding to $Re = 2400$, 3500 and 5000, respectively. (*d*) The perturbation kinetic energy varying with time from $t = 0$ to 4000 for the minimal seeds of 2-D plane Poiseuille flow for different Re. (The solid lines depict the chaotic transitional flow while the dashed lines depict the relaminarized flow.)

In Camobreco *et al.* (2023), the linear optimal disturbances with larger target time $8T_{opt}$ resemble the nonlinear optimal disturbances, and the leading adjoint mode represent the optimal initial disturbance in short channels. The linear optimal disturbances of $10T_{opt}$ are calculated with the energy gain 3.67. The linear optimal disturbances are still uniformly distributed in the channel and very similar to those of T_{opt} (see figure 3*a*). Figure 2(*b*) shows the comparison of energy time variation, the initial energy of $10T_{opt}$ is approximately 2.3831×10^{-4}, which is much smaller than 4.076684×10^{-4} for T_{opt}. Moreover, the uniform linear optimal disturbances reach the same edge state with the same energy, which is larger than that of the minimal seed. The linear optimal disturbances with larger target time are more efficient in triggering transitional flow than those of maximal energy growth; it is consistent with Camobreco *et al.* (2023) since the leading adjoint eigenmode is a more efficient initial condition and plays a very important role for larger target time. Moreover, the initial energy is still larger than the energy near the edge state, which means that the energy is not amplified compared with the initial energy. Figure 2(*c*) shows the energy time variation of minimal seeds for different Re, in this

study, the subcritical transitional flow could be observed as $Re \geqslant 2400$ for $\alpha = 0.1$. The critical initial energies are $E_0 = 4.922 \times 10^{-4}$ and $E_0 = 2.6186 \times 10^{-6}$ for $Re = 2400$ and 5000, respectively. The linear optimal disturbance could not induce the subcritical transitional flow for $Re = 2400$; while it requires $E_0 = 1.63153 \times 10^{-4}$ of linear optimal disturbance at $Re = 5000$ to trigger the transitional flow. It can be concluded that the critical initial energy of nonlinear optimal disturbance is less than 2.5 % of that of linear optimal disturbance with target time T_{opt}. To check if the minimal seeds could sustain the transitional flow after the target time $T = 2000$, figure 2(*d*) shows the variation of disturbance energy with respect to time from 0 to 4000 for different Re. The sustained transitional flow induced by the minimal seeds could be observed after the target time $T = 2000$.

At $Re = 5000$, the initial perturbation energy increases rapidly to the peak by the Orr mechanism, then it decreases gradually to the energy plateau related to the nonlinear edge state, the nonlinear evolution sustains along the basin boundary with a sufficiently long period before it drives the flow into chaotic transitional flow, in figures 2(*c*) and 2(*d*). The energy time variation is almost the same as that of $E_0 > E_D$ in figure 2(*a*) of Camobreco *et al.* (2023), which demonstrates that the subcritical transition mechanism (nonlinear TS waves) in 2-D plane Poiseuille flow is captured. Fully developed turbulence in 2-D plane Poiseuille flow has been observed when the Reynolds number is far beyond the critical value Re_c (Falkovich & Vladimirova 2018; Markeviciute & Kerswell 2021), which indicates that it might not be achieved if the Reynolds number is not greater than 5772.2 for 2-D plane Poiseuille flow. Therefore, it is not surprising that the obvious turbulent kinetic energy oscillation is absent in 2-D flow transitional flow, and the fully developed turbulence is absent for $Re < Re_c$. As Re decreases, the nonlinear optimal disturbances with increased initial kinetic energy could still trigger 2-D subcritical transitional flow, and the perturbation energy variation is the same as $Re = 5000$. By employing nonlinear optimizations, the subcritical transition of 2-D plane Poiseuille flow could be captured at $Re = 2400$. It is interesting that the energy growth at the peak for the nonlinear optimal disturbances is much smaller than the linear optimal disturbances, which might be attributed to the long target time and nonlinear interactions. For example, the maximum energy growth of linear optimal disturbance is approximately 34.08 for $Re = 3500$, while the maximum energy growth at the peak in only approximately 15.1. Moreover, the perturbation energy of the nonlinear edge state is smaller than the energy peak by Orr amplification for larger Re; while the energy of the edge state is slightly larger than the energy peak for $Re = 2400$. The kinetic energy of the transitional flow increases with Re.

Figure 3 compares the subcritical transitional flow field triggered by linear optimal disturbances and minimal seeds, represented by disturbance vorticity. The linear optimal disturbances distribute near the channel walls uniformly and symmetrically against the mean shear and filled in the whole channel, that are the wall mode. While the streamwise clustered nonlinear optimal disturbances locate one third of the channel, and the magnitude of nonlinear optimal disturbances is much smaller. The linear optimal disturbances are amplified by a tilting effect (see figure 3*a*,*b*); the linear travelling waves are formulated and the disturbance magnitude decreases (see figure 3*c*,*d*) uniformly; the disturbance magnitude decreases further non-uniformly and nonlinearly (see figure 3*e*,*f*); the decrease of magnitude ceases and the nonlinear TS waves are sustained (see figure 3*f*–*h*) before the chaotic transitional flow is reached.

Unlike the linear optimal disturbances, the nonlinear optimal disturbances are streamwise localized wave packets and not symmetric due to the nonlinear interaction in the optimization. The localized optimal disturbances are amplified by the Orr mechanism
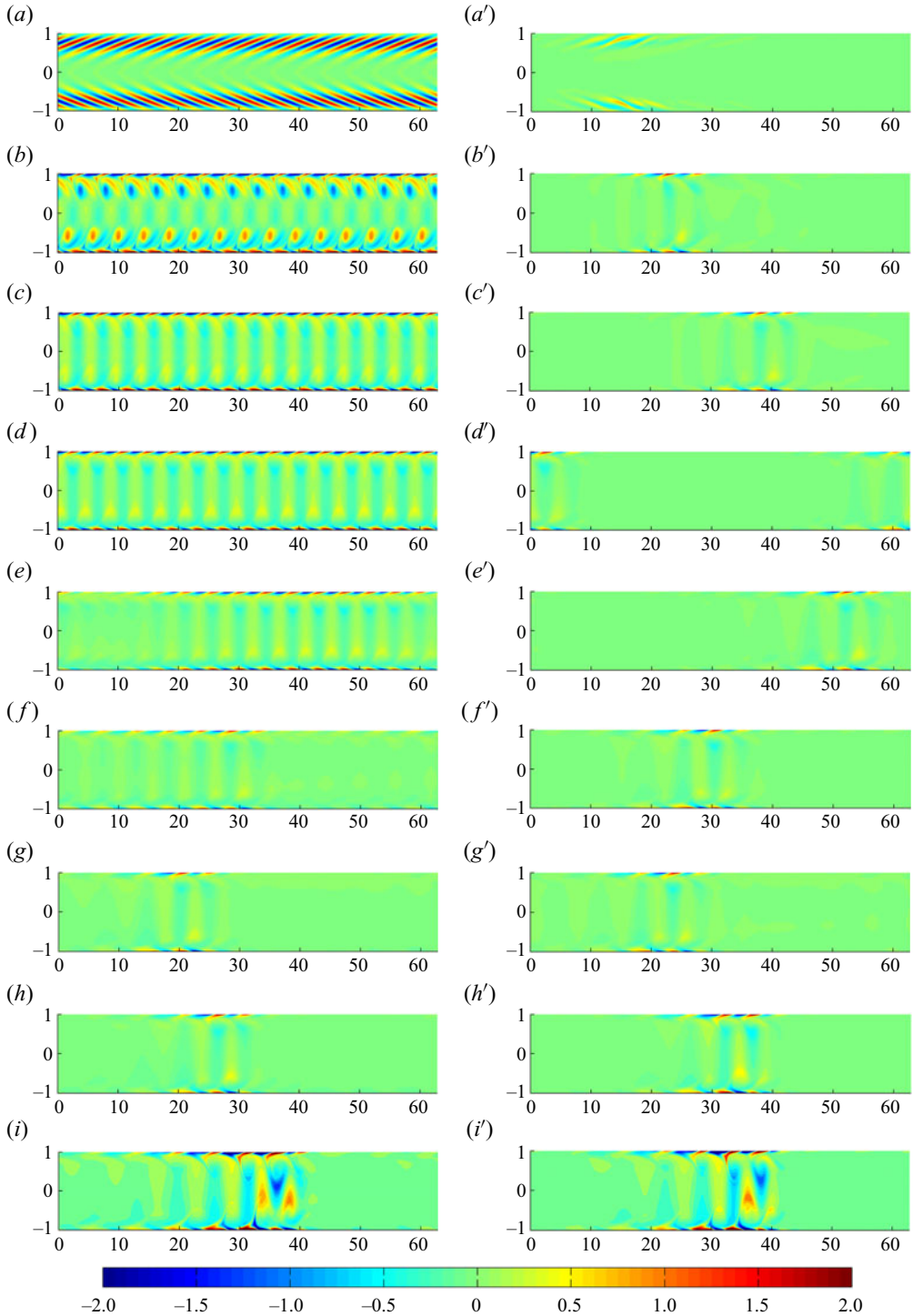
Figure 3. The comparison of vorticity snapshots in the subcritical transition triggered by the (*a–i*) linear and (*a′–i′*) nonlinear optimal disturbances for 2-D plane Poiseuille flow at $Re = 3500$. The time instants for snapshots, (*a–i*) and (*a′–i′*), are $t = 0, 20, 50, 100, 200, 400, 1000, 1500$ and 2000, respectively.

to obey the mean shear (figure 3b'), and the nonlinear interactions are evoked immediately to form the nonlinear TS waves (figure 3c'). The nonlinear TS waves and the nonlinear edge state sustains for a sufficiently long time, before the fluid-structure deviates into the 2-D chaotic transitional state (figure 3i'). From the vorticity distributions, we can see that the flow induces unsteadiness of the sharp vortex sheets ejected from the wall by the nonlinear travelling waves, and is mediated by the secondary updrafts induced at the walls by vorticity inhomogeneities in the core of the channel, which is consistent with the observations (Jiménez 1990). Interestingly, the fluid structures are very similar after $t = 400$ for both the linear (figure 3f–i) and nonlinear (figure 3f'–i') disturbances. It indicates that the linear optimal disturbances could be treated as candidate to investigate the subcritical transition of shear flows (Camobreco *et al.* 2023), since the nonlinear TS waves along the linear edge state are very similar to the nonlinear edge state. It should be noted that most of the uniform distributed linear optimal disturbances are decayed. If only parts of disturbances in the channel are considered, the required initial energy density might be reduced. For example, if the first half of the channel is filled with disturbances and then zeroed everywhere outside of the first half, e.g. filtered with a step function, then the initial energy density of the linear optimal is reduced to 1.11882×10^{-4}, compared with 4.076684×10^{-4} for the linear optimal disturbances without applying a step function and 9.24967×10^{-6} for the nonlinear optimal disturbances. Therefore, quantitatively, the minimal seeds capture the edge state more efficiently for long channels.

4. The wall mode optimal disturbance for subcritical transition

The optimal disturbances are amplified by the Orr mechanism in 2-D plane Poiseuille flow. However, the magnitude of the streamwise velocity perturbation is much larger than that of vertical velocity perturbation. In this section, the quantitative relation between the two perturbation components is investigated. Figure 4 shows the time variation of the perturbation energy of velocity components and their ratio for the optimal disturbances. The time variation of perturbation energy of streamwise velocity E_u shows the same trend as the total kinetic energy (see figure 2a) for different Re, while the variations of E_v are quite different from E_u. It is obvious that the perturbation energy of streamwise velocity u is much larger than the vertical velocity v, which means the streamwise velocity is predominant in the 2-D flow. Correspondingly, the amplification of E_v is much more remarkable than that of E_u, since the initial energy norm E_v is much smaller. From figure 3, the initial optimal disturbances are located near the channel wall. According to the well-established linear instability and transient growth theories (Lin 1944; Drazin & Reid 1981; Trefethen *et al.* 1993; Schmid & Henningson 2001; Chapman 2002; Schmid 2007), the wall mode disturbances of the linearized NS equations (Orr–Sommerfeld equations) of 2-D plane Poiseuille flow locate near the channel walls. Here, the uniformly disturbed linear optimal disturbances are the wall mode as shown in figure 3(a). For the wall mode near the channel wall $y = -1$, there exists the scaling law (Lin 1944; Chapman 2002)

$$y = -1 + y'/(\alpha Re)^{1/3}, \tag{4.1}$$

where y' is the scaled coordinate variable near the channel wall. Instead of the rigorous but time-consuming asymptotic analysis in Chapman (2002), we just focus the continuity equation $u_x + v_y = 0$ for estimation since there are no disturbances near the channel centre. According to the periodic boundary condition in the streamwise direction, the
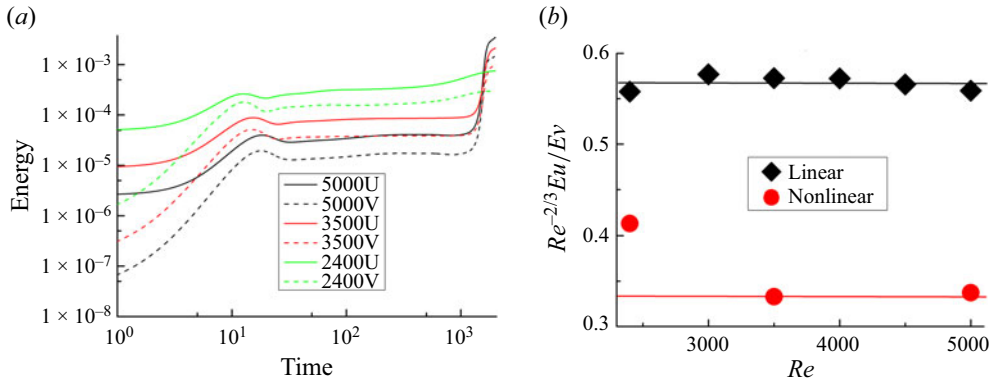
Figure 4. The time variation of perturbation energy of velocity components (*a*) and the ratios between the optimal disturbances (*b*) in 2-D plane Poiseuille flow at different *Re*.

disturbances could be decomposed into Fourier modes, such as

$$v(x, y) = \sum \tilde{v}(y) \exp^{i\alpha x}, \tag{4.2}$$

where $\tilde{v}(y)$ are continuous functions in the wall-normal direction. Therefore,

$$i\alpha\tilde{u}(y) + d\tilde{v}(y)/dy = 0 \tag{4.3}$$

is obtained according to the continuity equation. Considering the wall modes and the scaling (4.1), $i\alpha\tilde{u}(y')$ should be balanced by $d\tilde{v}(y')/dy'(\alpha Re)^{1/3}$ near the channel wall. Consequently, it can be concluded that E_u is approximately $(Re)^{2/3}E_v$ for the wall mode optimal disturbances if one focuses on the fixed streamwise wavenumber. Figure 4(*b*) presents the values of $(Re)^{-2/3}E_u/E_v$ varying with *Re* for the linear optimal disturbances in 2-D plane Poiseuille flow. The values are almost constant, i.e. 0.567 ± 0.01, which demonstrates the linear optimal disturbances are the wall modes, quantitatively. However, for the minimal seeds that induce the subcritical transitional flow, the values of $(Re)^{-2/3}E_u/E_v$ are much smaller, which might be the reason why the peak energy amplification is much smaller. The value keeps constant at approximately 0.33 for large Reynolds numbers, while it is 0.41 at $Re = 2400$. It might be concluded that minimal seeds are also exact wall modes for large *Re*, although they are streamwise localized in the channel; the nonlinear optimal disturbances deviate the wall mode to trigger subcritical transitional flow.

Figure 5 compares the initial optimal disturbances represented by disturbance streamwise velocity and the disturbance vorticity. Generally, the value of the vorticity is approximately one order larger than the value of the streamwise velocity. According to the definition of vorticity $\omega = u_y - v_x$ and the asymptotic scaling of the wall mode, it is very reasonable to obtain these results. For the nonlinear optimal disturbances, the initial value of streamwise velocity and vorticity decreases with *Re*. Moreover, the disturbance distributions are very similar between $Re = 3500$ and $Re = 5000$, while the disturbances are more distorted for $Re = 2400$. It should be noted that the values of streamwise velocity and vorticity for the linear optimal disturbances $E_0 = 4.076686 \times 10^{-4}$ (see figure 5*a*,*a'*) are only approximately twice of those of the minimal seeds $E_0 = 9.24967 \times 10^{-6}$ (see figure 5*c*,*c'*) at $Re = 3500$. The streamwise localization makes the minimal seeds much more efficient to trigger the subcritical transitional flow, since the strong nonlinear interactions are fully considered including the Orr amplification and edge states.
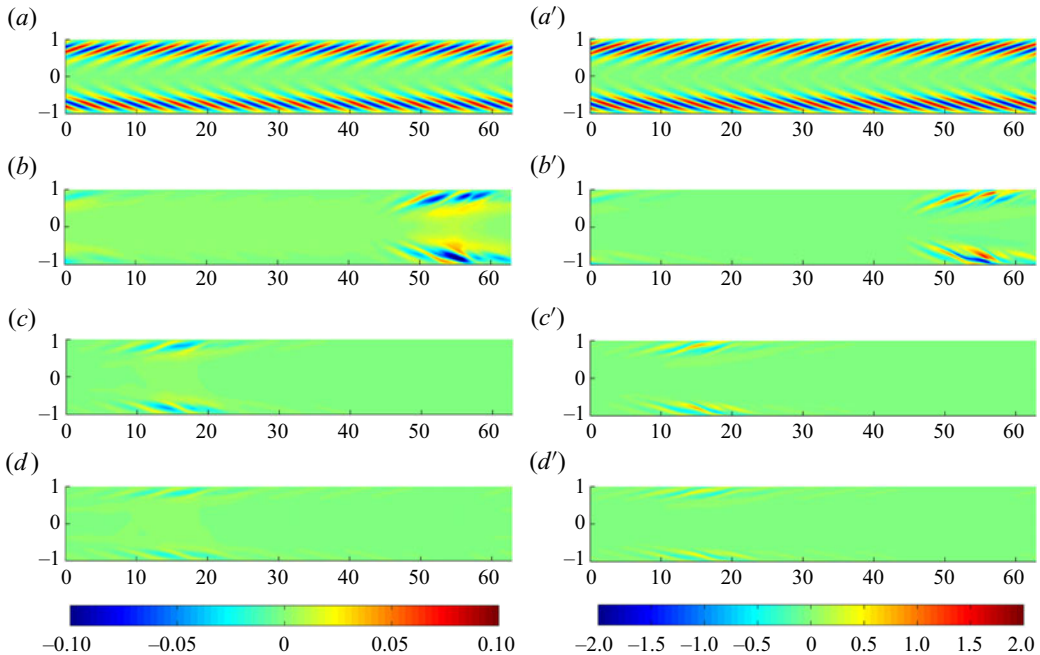
994 A6-10

Figure 5. The comparison of streamwise velocity of (*a–d*) and vorticity (*a′–d′*) optimal disturbances in 2-D plane Poiseuille flow at different *Re*. Panels (*a,a′*), (*b,b′*), (*c,c′*) and (*d,d′*) show the results for *Re* = 3500, 2400, 3500 and 5000, respectively. Panels (*a,a′*) show the linear initial optimal disturbances, while (*b,b′*), (*c,c′*) and (*d,d′*) show the nonlinear initial optimal disturbances.

5. Discussion and conclusions

The subcritical transition to turbulence for 3-D shear flows has been extensively investigated, and the optimal disturbances would generate streaks (Monokrousos *et al.* 2011; Eaves & Caulfield 2015) with small initial energy or hairpin vortices (Karp & Cohen 2014; Farano *et al.* 2015*a*) with sufficient initial energy to trigger the turbulence. The nonlinear non-modal instability based on nonlinear optimizations could capture the minimal seeds that evolve along the edge state before transition to turbulence, because the nonlinear optimal disturbances are amplified by both the Orr and lift-up effects and it is very suitable for studying the critical subcritical transitional shear flows quantitatively. However, for quasi-2-D flows or 2-D flows, the disturbances are amplified by only the vortex tilting effect due to the strong suppression of the lift-up effect, while the nonlinear transient growth and the mechanism of subcritical transition to turbulence has remained unclear. Recently, Camobreco *et al.* (2023) employed the linear optimal disturbances to touch the edge state successfully, and revealed that the subcritical transition to turbulence is caused by the nonlinear TS mechanism in the quasi-2-D shear flows encountered in magnetohydrodynamic flow. However, the same edge state had been reached by nonlinear and linear optimal disturbances with different initial energy and target time (Camobreco *et al.* 2023). Recall that, the nonlinear edge state usually is achieved by the minimal seed named as the optimal disturbances with the minimal energy that trigger subcritical transition to turbulence (Pringle *et al.* 2012). Therefore, it is urgently needed to clarify if the linear and nonlinear optimal disturbances are similar in subcritical transitional flow in 2-D shear flows. In this paper, we studied the subcritical transitional flow in 2-D plane Poiseuille flow by extensive numerical simulations, and the channel with length

20π is chosen to check the streamwise localization on nonlinear optimal disturbances (Mellibovsky & Meseguer 2015).

The edge state is reached by the linear optimal disturbance and minimal seeds. However, the energy norms of the two edge states are quantitatively different, and the initial energy of minimal seeds is significant smaller than that of linear optimal disturbances. The strong chaotic transitional flow is observed in the present study, as Re decreases to 2400. The minimal seeds distribute near the wall and are streamwise localized; and experience the Orr amplification nonlinearly to achieve the maximal energy growth before reaching the edge state; finally the strong chaotic flow, a precursor to turbulence, is achieved. The evolution is very similar to that in Camobreco *et al.* (2023) except the sustained small-scale turbulence, whose Reynolds number $Re = 71\,211$. Moreover, it is not surprising that the fully sustained turbulence requires $Re > 30\,000$ for 2-D plane Poiseuille flow (Falkovich & Vladimirova 2018). Interestingly, the energy of the edge state is smaller than the achieved maximal energy for high Re. Moreover, the minimal seed conforms to the wall mode disturbance for high Re.

To trigger the turbulence in 2-D and quasi-2-D flows is of great interest in high efficient electron flows (Sulpizio *et al.* 2019) and laboratory experiments with soap films. This study suggests that the localized disturbances near the channel walls could be favourable in triggering the subcritical transitional flow in the 2-D shear flows.

Declaration of interests. The authors report no conflict of interest.

Author ORCID.

Z. Huang https://orcid.org/0000-0001-8000-6039.

REFERENCES

BOFFETTA, G. & ECKE, R.E. 2012 Two-dimensional turbulence. *Annu. Rev. Fluid Mech.* **44** (1), 427–451.

BUTLER, K.M. & FARRELL, B.F. 1992 Three-dimensional optimal perturbation in viscous shear flow. *Phys. Fluids* A **4**, 1637–1650.

CAMOBRECO, C.J., POTHÉRAT, A. & SHEARD, G.J. 2021 Transition to turbulence in quasi-two-dimensional MHD flow driven by lateral walls. *Phys. Rev. Fluids* **6** (1), 013901.

CAMOBRECO, C.J., POTHÉRAT, A. & SHEARD, G.J. 2023 Subcritical transition to turbulence in quasi-two-dimensional shear flows. *J. Fluid Mech.* **963**, R2.

CHAPMAN, S.J. 2002 Subcritical transition in channel flows. *J. Fluid Mech.* **451**, 35–97.

CHERUBINI, S. & PALMA, P.D. 2015 Minimal-energy perturbations rapidly approaching the edge state in Couette flow. *J. Fluid Mech.* **764**, 572–598.

CHERUBINI, S., PALMA, P.D., ROBINET, J.C. & BOTTARO, A. 2011 The minimal seed of turbulent transition in the boundary layer. *J. Fluid Mech.* **689**, 221–253.

DAVIS, S.J. & WHITE, C.M. 1928 An experimental study of the flow of water in pipes of rectangular sections. *Proc. R. Soc. Lond.* A **119**, 92–107.

DRAZIN, P.G. & REID, W.H. 1981 *Hydrodynamic Stability*. Cambridge University Press.

EAVES, T.S. & CAULFIELD, C.P. 2015 Disruption of SSP/VWI states by a stable stratification. *J. Fluid Mech.* **784**, 548–564.

FALKOVICH, G. & VLADIMIROVA, N. 2018 Turbulence appearance and nonappearance in thin fluid layers. *Phys. Rev. Lett.* **121**, 164501.

FARANO, M., CHERUBINI, S., ROBINET, J.C. & PALMA, P.D. 2015*a* Hairpin-like optimal perturbations in plane Poiseuille flow. *J. Fluid Mech.* **775**, R2.

FARANO, M., CHERUBINI, S., ROBINET, J.C. & PALMA, P.D. 2015*b* Subcritical transition scenarios via linear and nonlinear localized optimal perturbations in plane Poiseuille flow. *Fluid Dyn. Res.* **48**, 061409.

HACK, P.M.J. & MOIN, P. 2017 Algebraic disturbance growth by interaction of Orr and lift-up mechanisms. *J. Fluid Mech.* **829**, 112–126.

HUANG, Z. & PHILIPP, M.J.H. 2020 A variational framework for computing nonlinear optimal disturbances in compressible flows. *J. Fluid Mech.* **894**, A5.

JIMÉNEZ, J. 1987 Bifurcations and bursting in two dimensional Poiseuille flow. *Phys. Fluids* **30**, 3644–3646.

JIMÉNEZ, J. 1990 Transition to turbulence in two-dimensional Poiseuille flow. *J. Fluid Mech.* **218**, 265–297.

KARP, M. & COHEN, J. 2014 Tracking stages of transition in Couette flow analytically. *J. Fluid Mech.* **748**, 896–931.

KERSWELL, R.R. 2018 Nonlinear nonmodal stability theory. *Annu. Rev. Fluid Mech.* **50**, 319–345.

LIN, C.C. 1944 On the development of turbulence. PhD thesis, California Institute of Technology.

MARKEVICIUTE, V.K. & KERSWELL, R.R. 2021 Degeneracy of turbulent states in two-dimensional channel flow. *J. Fluid Mech.* **917**, A57.

MELLIBOVSKY, F. & MESEGUER, A. 2015 A mechanism for streamwise localisation of nonlinear waves in shear flows. *J. Fluid Mech.* **779**, R1.

MONOKROUSOS, S., BOTTARO, A., BRANDT, L., DI VITA, A. & HENNINGSON, D.S. 2011 Nonequilibrium thermodynamics and the optimal path to turbulence in shear flows. *Phys. Rev. Lett.* **106**, 134502.

ORSZAG, S.A. 1971 Accurate solution of the Orr–Sommerfeld equation. *J. Fluid Mech.* **50**, 689–703.

PRINGLE, C.C.T. & KERSWELL, R.R. 2010 Using nonlinear transient growth to construct the minimal seed for shear flow turbulence. *Phys. Rev. Lett.* **105**, 154502.

PRINGLE, C.C.T., WILLIS, A.P. & KERSWELL, R.R. 2012 Minimal seeds for shear flow turbulence: using nonlinear transient growth to touch the edge of chaos. *J. Fluid Mech.* **702**, 415–443.

RABIN, S.M.E., CAULFIELD, C.P. & KERSWELL, R.R. 2012 Triggering turbulence efficiently in plane Couette flow. *J. Fluid Mech.* **712**, 244–272.

REDDY, S.C., SCHMID, P.J., BAGGETT, J.S. & HENNINGSON, D.S. 1998 On stability of streamwise streaks and transition thresholds in plane channel flows. *J. Fluid Mech.* **365**, 269–303.

REYNOLDS, O. 1883 An experimental investigation of the circumstances which determine whether the motion of water shall be direct or sinuous and of the law of resistance in parallel channels. *Phil. Trans. R. Soc. Lond.* **174**, 935–982.

ROIZNER, F., KARP, M. & COHEN, J. 2016 Subcritical transition in plane Poiseuille flow as a linear instability process. *Phys. Fluids* **28**, 054104.

SCHMID, P.J. 2007 Nonmodal stability theory. *Annu. Rev. Fluid Mech.* **39**, 129–162.

SCHMID, P.J. & HENNINGSON, D.S. 2001 *Stability and Transition in Shear Flows*. Springer.

SULPIZIO, J.A., ELLA, L., ROZEN, A., BIRKBECK, J., PERELL, D.J., DUTTA, D., BEN-SHALOM, M., TANIGUCHI, T., WATANABE, K. & HOLDER, T. 2019 Visualizing Poiseuille flow of hydrodynamic electrons. *Nature* **576** (7785), 75–79.

TAYLOR, J.R. 2008 Numerical simulations of the stratified oceanic bottom boundary layer. PhD thesis, University of California, San Diego.

TILLMARK, N. & ALFREDSSON, P.H. 1992 Experiments on transition in plane Couette flow. *J. Fluid Mech.* **235**, 89–102.

TREFETHEN, L.N. & EMBREE, M. 2005 *Spectra and Pseudospectra: The Behavior of Nonnormal Matrices and Operators*. Princeton University Press.

TREFETHEN, L.N., TREFETHEN, A.E., REDDY, S.C. & DRISCOLL, T.A. 1993 Hydrodynamic stability without eigenvalues. *Science* **261**, 578–584.

ZAMMERT, S. & ECKHARDT, B. 2014 Streamwise and doubly-localised periodic orbits in plane Poiseuille flow. *J. Fluid Mech.* **761**, 348–359.

ZAMMERT, S. & ECKHARDT, B. 2019 Transition to turbulence when the Tollmien–Schlichting and bypass routes coexist. *J. Fluid Mech.* **880**, R2.